

Centre for Archaeology Report 9/2005

**Luminescence Dating for the Bletchingley Excavations,  
Surrey**

Dr P S Toms

© English Heritage 2005

ISSN 1473-9224

*The Centre for Archaeology Report Series incorporates the former Ancient Monuments Laboratory Report Series. Copies of Ancient Monuments Laboratory Reports will continue to be available from the Centre for Archaeology (see back cover for details).*

## Luminescence Dating for the Bletchingley Excavations, Surrey

Dr P S Toms

### Summary

Three conventional sediment samples and six burnt flints obtained from section A11 of the Bletchingley excavations were submitted for optical and thermoluminescence dating, respectively, by English Heritage. An attempt to quantify the accuracy of all luminescence age estimates was made using signal analysis methods to detect partial resetting of datable signals prior to sample interment, and through consideration of the influence of varying moisture content and cosmic dose rate over the burial period. Optical dating evolved a chronology of sedimentation, not necessarily continuous, from c 32ka (30,000 BC) through to c 2.8 ka (800 BC). Three flints were excluded from the study owing to evidence of insufficient heating prior to burial. The remaining flints, located in close proximity to each optical dating sample, generated age estimates of c 7 to 12 ka (5000 to 10,000 BC) consistent with age expectations premised upon microliths recovered from equivalent levels across the site. However, a significant inversion in age between the lowermost optical dating sample and the underlying flint sample was recorded. After considering the accuracy of  $D_e$  and dose rate estimates for both sample types, this anomaly was attributed to displacement of the flint samples from its primary context by anthropogenic activity or gravitational effects coupled with low adhesion afforded by the sand matrix within which all the flint samples were located. Similar displacement, for all the flint samples that have yielded age estimate in this study, cannot be dismissed. The juxtaposition of Mesolithic burnt flints and Iron Age sediments and charcoal in the uppermost dated unit evidences a period of land surface stability and repeated human occupation of this area.

### Keywords

Luminescence Dating  
Geochronology

### Author's address

Geochronology Laboratories, School of Environment, University of Gloucestershire,  
Swindon Road, Cheltenham GL50 4AZ. Telephone: 01242 544091. Email: ptoms@glos.ac.uk

*Many CfA reports are interim reports which make available the results of specialist investigations in advance of full publication. They are not subject to external refereeing, and their conclusions may sometimes have to be modified in the light of archaeological information that was not available at the time of the investigation. Readers are therefore advised to consult the author before citing the report in any publication and to consult the final excavation report when available.*

*Opinions expressed in CfA reports are those of the author and are not necessarily those of English Heritage.*

## 1.1 Preamble

Luminescence ages are premised upon,

- i) the reduction of the datable signal - thermo- or optically stimulated luminescence - within naturally occurring minerals to zero through exposure to heat or sunlight, and once buried,
- ii) the re-accumulation of this signal by exposure to natural radiation existent within surrounding sediments, emanating from the cosmos and/or located within the mineral grains to be dated.

If the amount of luminescence accrued is directly proportional to the total dose absorbed by minerals since burial then the age of final firing or sedimentation can be estimated using the expression,

$$\text{Age} = \frac{\text{Mean Total dose}}{\text{Mean Total Dose Rate}}$$

## 1.2 Sample details

Sampled Section	Sample field code	Sample Type	UGGL code	Depth (m)	Altitude (m)	Latitude (°N)	Longitude (°E)
A11	A11/3	Sediment	GL03109	0.59	110	51	0
	A11/2	Sediment	GL02110	1.35			
	A11/1	Sediment	GL03111	1.55			
	-	Burnt Flint	GL03112	0.65-0.70			
	-	Burnt Flint	GL03113				
	-	Burnt Flint	GL02114	1.00-1.05			
	-	Burnt Flint	GL03115	1.60-1.65			
	-	Burnt Flint	GL03116				
	-	Burnt Flint	GL03117				

Table 1 Optical and thermoluminescence dating sample codes and location details, Bletchingley.

## 2.0 Methodology

### 2.1 Sample collection

Three conventional sediment samples (Table1; Fig 1) – those located within units composed predominantly of sand and silt – were collected in daylight from section A11 of excavations at North Park Farm, Bletchingley, Surrey (TQ330520), by means of opaque

plastic tubing (150x45 mm) forced into the sediment face. Each sediment sample was wrapped in clingfilm and parcel tape in order to preserve moisture content and integrity until ready for laboratory preparation. Additional moisture content samples were collected from the rear of the cavity created by sampling and insertion of a gamma spectrometer. These were double-bagged, again to maintain that moisture content existent within each unit at the time of sampling.

Six samples of burnt flint were recovered from three bulk samples, obtained from three levels within section A11 (Table 1; Fig 1), by Archaeoscape Consulting (Royal Holloway, University of London). These samples were submitted for dating wrapped in aluminium foil in order to avoid optical erosion of the datable signal (Huxtable 1981). Each was accompanied, in separate single bags, by respective sub-samples of raw sediment from each bulk sample.

## **2.2 Sample preparation**

All samples were processed under controlled laboratory lighting conditions provided by Encapsulite RB-10 (red) filters in order to preclude optical erosion of the time dependent signal.

### **2.2.1 Sediment samples**

To isolate that material potentially exposed to daylight during sampling, sediment located within 20 mm of each tube-end was removed. These 'end' samples along with the remaining 'core' and separate moisture content samples were assessed individually for moisture content in order to examine the consistency of this value. In the event of a discrepancy in these estimates, perhaps brought about by surface drying, the maximum value was incorporated into the calculation of dose rate.

The 'core' content of each sample was dried at 40°C for 48 hours and then dry sieved. Quartz within the fine sand (125-180 µm) fraction was then isolated (Table 2). This fraction was treated with 10% hydrochloric acid (HCl) and 10% hydrogen peroxide (H<sub>2</sub>O<sub>2</sub>) to attain removal of carbonate and organic components. These samples were then etched for 60 mins in 40% hydrofluoric acid (HF), in order to remove the outer 10-15 µm layer affected by alpha radiation and degrade each samples' feldspar content. Whilst in HF, each sand sample was continuously stirred using a magnetic stirrer and follower apparatus in an

attempt to achieve isotropic etching of grains. 10% hydrochloric acid was then added to remove acid soluble fluorides. Each sample was dried, resieved, and quartz isolated from the remaining heavy mineral fraction using a sodium polytungstate density separation at  $2.68 \text{ g.cm}^{-3}$ . Twelve multi-grain aliquots (c 6 mg, 4000 grains) of quartz from each sample were then mounted on aluminium discs for the determination of equivalent dose values.

Quartz was used as the minerogenic dosimeter primarily because of the stability of its datable signal over the mid to late Quaternary period, predicted through isothermal decay studies (eg Smith *et al* 1990; retention lifetime 630 Ma at 20°C) and evidenced by optical age estimates concordant with independent chronological controls (Wallinga *et al* 2001; Murray *et al* 2002; Murray and Olley 2002; Stokes *et al* 2003; Watanuki *et al* submitted). This stability is in contrast to the anomalous fading of comparable signals commonly observed for other ubiquitous sedimentary minerals such as feldspar and zircon (Wintle 1973; Templer 1985; Spooner 1993).

### **2.2.2 Burnt flint samples**

Each flint sample exhibited external evidence, in the form of a reddened or fractured surface, of possible exposure to heat in the past. The external layer of each flint sample, of minimum thickness 2 mm, was removed using a vice-crushing apparatus to eliminate that material exposed to alpha and beta radiation generated within the surrounding sediment. The remaining core of each sample was then crushed using an agate pestle and mortar and dry sieved. Flint within the fine sand (125-180  $\mu\text{m}$ ) fraction was then treated with 10% hydrochloric acid to remove carbonate components (Valladas 1978). The limited size of each flint sample restricted the datable mass of each 125-180  $\mu\text{m}$  fraction to c 50 mg. Eight ~6 mg aliquots of each flint sample were then mounted on aluminium discs for the determination of equivalent dose values.

## **2.3 Equivalent Dose ( $D_e$ ) acquisition**

Conventional luminescence measurements, generating  $D_e$  values from multi-grain aliquots, were made using an automated TL-DA-15 Risø set (Markey *et al* 1997).

### **2.3.1 Sediment samples**

Optical stimulation of luminescence was provided by a 150 W tungsten halogen lamp, filtered to a broad blue-green light, 420-560 nm (2.21-2.95 eV) conveying  $16 \text{ mWcm}^{-2}$ ,

using three 2 mm Schott GG420 and a broadband interference filter. Infrared stimulation, provided by 13 IR diodes (Telefunken TSHA 6203) stimulating at  $875\pm 80\text{nm}$  delivering  $\sim 5\text{ mWcm}^{-2}$ , was used to indicate the presence of contaminant feldspars (Hütt *et al* 1988). This diagnostic, applied to both the natural and laboratory signals (to accommodate potential fading of IRSL signals), indicated such contamination to be absent from aliquots of each sample. Stimulated photon emissions from the quartz aliquots were filtered by 5 mm of HOYA U-340 glass filters.

All (UV) emissions were detected by an EMI 9235QA photomultiplier fitted with a blue-green sensitive alkali photocathode. Regenerated optical signals were obtained by irradiation using a 40 mCi  $^{90}\text{Sr}/^{90}\text{Y}$  beta source incorporated within the Risø set and calibrated for 125-180  $\mu\text{m}$  multi-grain aliquots of quartz against the 'Hotspot 800'  $^{60}\text{Co}$  gamma source located at the National Physical Laboratory, UK.

$D_e$  values were obtained through calibrating the 'natural' optical signal (Fig 2, *left column*), acquired during burial, against 'regenerated' optical signals obtained by administering known amounts of laboratory dose. Specifically,  $D_e$  estimates were obtained using a Single-Aliquot Regenerative-dose (SAR) protocol, similar to that proposed by Murray and Wintle (2000; 2003).

Up to five different regenerative-doses were administered so as to image dose response, defining that portion of linear response bracketing the natural signal from which  $D_e$  values were interpolated and associated errors (counting and fitting) calculated by way of linear regression (Green and Margerison 1978; Fig 2, *inset left column*). To secure comparability between environmental and laboratory induced signals, preheating of each aliquot prior to measurement of natural and regenerated signals was  $260^\circ\text{C}$  for 10 s. A test dose of 5 Gy, followed by preheating at  $220^\circ\text{C}$  for 10 s, was used in monitoring and correcting for sensitivity change resulting from the process of  $D_e$  acquisition. Optical stimulation of each aliquot occurred at  $125^\circ\text{C}$  in order to minimise effects associated with photo-transferred thermoluminescence and maximise signal to noise ratios.

The ratio of repeat regenerative-doses (approximating  $D_e$  values) was obtained for each aliquot in order to clarify the success of sensitivity correction. Repeat ratios approximating unity, as in the case of samples in the present study – 0.99-1.04 ( $1.01\pm 0.03$ ,  $1\sigma$  standard deviation) – are taken as indicative of accurate sensitivity correction. Zero-dose signal

response was used as a measure of thermal transfer relating to test dose preheating and subtracted from regenerative-dose responses.  $D_e$  values were accepted if their associated error was  $\leq 20\%$ . Mean  $D_e$  values, given in Table 2, are the weighted (geometric) mean  $D_e$  calculated using the central age model outlined by Galbraith *et al* (1999) and are quoted at  $1\sigma$  confidence (standard error).

### 2.3.2 Burnt flint samples

Thermoluminescence (TL) was stimulated through heating aliquots to  $500^\circ\text{C}$  at  $2^\circ\text{Cs}^{-1}$  in a Nitrogen atmosphere (pumped at  $1 \text{ l}\cdot\text{min}^{-1}$ ). Thermally stimulated photon emissions from the flint aliquots were filtered by 2 mm Schott BG39 and Corning 7-59 glass filters. Filtered emissions were detected by an EMI 9235QA photomultiplier fitted with a blue-green sensitive bi-alkali photocathode. Additive-dose thermoluminescence signals were induced by irradiation from the same 40 mCi  $^{90}\text{Sr}/^{90}\text{Y}$  beta source outlined in section 2.3.1 and calibrated for 125-180  $\mu\text{m}$  flint against the 'Hotspot 800'  $^{60}\text{Co}$  gamma source.

$D_e$  values were obtained through comparing the 'natural' thermal signal, acquired during burial, and the 'additive' thermal signal (Figs 3 and 4, *left columns*) obtained by administering known amounts of laboratory dose to aliquots containing a natural signal (Figs 3 and 4, *right columns*). Specifically,  $D_e$  estimates were obtained using a Multiple-Aliquot Additive-Dose (MAAD) protocol, similar to that outlined by Mercier *et al* (1995). From a set of six aliquots, the natural signal was measured from one with the remainder exposed to five different additive-doses so as to define dose response in excess of the natural signal. Thermal signals were integrated between  $350^\circ\text{C}$  and  $400^\circ\text{C}$ , exploiting the temporal stability of the signal associated with the  $380^\circ\text{C}$  TL peak (50 Ma retention lifetime; Wintle and Aitken 1977; Bowman 1982). Background TL was measured and subtracted from this integral. Inter-aliquot normalisation, accounting for potential differences in mass and/or signal sensitivity between aliquots, was achieved by utilising the signal response (less background response) of each aliquot to a standard dose of 10 Gy. The  $D_e$  value for each sample was obtained through extrapolation of dose equating to zero signal response using the measured response defined by additive and natural dose points fitted with either an unweighted single saturating exponential or, in the event of sub-linear dose response, a second order polynomial (Figs 3 and 4, *right column*). The natural TL signal of a further two aliquots was thermally reset (through heating to  $500^\circ\text{C}$ ) then given different laboratory doses, each less than the extrapolated  $D_e$  value, to examine the dose response of that signal accrued whilst buried in order to ensure that the extrapolated

dose response and  $D_e$  value were accurately defined. The natural TL signal from these aliquots was also incorporated into the dose response plot (Figs 3 and 4, *right column*) in order to further refine the extrapolation of  $D_e$ , presented in Table 2.

#### 2.4 Acquisition of dose rate value

Table 2 also details dose rate information. The total dose rate to quartz within each sediment sample represents the summed effect of external radiation sources, consisting of beta ( $\beta$ ) particles and gamma ( $\gamma$ ) photons emanating from within surrounding sediment, and muons and electrons streaming from the cosmos. Mean  $\gamma$  dose rate to each sediment sample has been derived from measurements of U, Th, and K concentrations collected *in situ* using an EG&G  $\mu$ Nomad portable NaI gamma spectrometer, calibrated using the block standards at RLHA, Oxford University. These *in situ* measurements of  $\gamma$  spectra reduce the uncertainty relating to potential heterogeneity in the  $\gamma$  dose field surrounding each sample. The mean  $\beta$  dose rate to each sediment sample was derived through quantifying radionuclide concentration within sub-samples of 'core' material. Owing to the low concentration of radionuclides within samples GL03110 and GL03111, evidenced through  $\gamma$  spectrometry, quantification of these was made by Inductively Coupled Plasma Mass Spectrometry (ICP-MS, supplied by School of Geography, Oxford University), offering the required parts per billion detection limits. Estimations of cosmic dose followed the calculations of Prescott and Hutton (1994); alteration in the thickness of overburden over the burial period, influencing the accuracy of such calculations, is considered in section 4. Dose rate calculations, following those described by Aitken (1985), incorporated dose rate conversion factors (Adamiec and Aitken 1998),  $\beta$ -attenuation factors (Mejdahl 1979), and the absorption coefficient of present water content (Zimmerman 1971), with an arbitrary 25% relative uncertainty attached in an attempt to accommodate temporal variations in past moisture content.

The rate of dose exposure to each flint sample reflects the sum of radiation both internal and external to each clast. Relevant internal radiation consists of alpha ( $\alpha$ ) and  $\beta$  particles generated by U, Th, and K constituents of each flint. Due to the often low concentration of these radionuclides within flint (Mercier *et al* 1995), their quantification was also made by ICP-MS assay. Radionuclide concentration was then converted into internal  $\alpha$  and  $\beta$  dose rates using those factors detailed by Valladas (1988) and Bell (1979) and an  $\alpha$ -sensitivity coefficient of  $0.10 \pm 0.02$ . Pertinent external radiation comprises  $\gamma$  photons evolved from

radionuclides within the surrounding sediment and cosmic derived muons and electrons. Mean  $\gamma$  dose rate to each flint was calculated from radionuclide concentrations, determined by ICP-MS assay of respective sediment samples submitted with each flint, using the dose rate conversion and absorption factors outlined above. Again, estimations of cosmic dose rate followed the calculations of Prescott and Hutton (1994).

## **2.5 Luminescence age acquisition**

Luminescence ages were obtained through dividing the mean  $D_e$  value by the mean total dose rate value and are shown in Table 2. The standard error on luminescence age estimates is quoted at  $1\sigma$  confidence and is premised upon the propagation of both systematic and experimental ( $1\sigma$ ) standard errors associated with those parameters, outlined above, contributing to the calculation of  $D_e$  and dose rate values. Figure 5 shows the composite probability mass function of age obtained for each sample, incorporating  $D_e$  and dose rate uncertainties for each aliquot along with the  $1\sigma$  standard error range about the mean age.

## **3.0 Assessment of accuracy**

The accuracy of age estimates presented in this study has been assessed within the context of the potential existence of residual datable signals subsequent to burial. This effect may be due to pre-burial exposure to an attenuated spectrum, intensity and/or period of sunlight in the case of sediment samples or an attenuated thermal regime for flint samples, and may manifest in the form of age overestimation. For both materials, signal analysis can assist in the detection of aliquots consisting of partially reset grains, leading to the production of an amended age or a maximum age estimate.

## **3.1 Sediment samples**

$D_e(t)$  plots proposed by Bailey (2003) for use in conjunction with SAR, exploit the existence of signal accumulation sites (traps) within minerogenic dosimeters that reset (bleach) with different efficiency for a given wavelength of light.  $D_e(t)$  plots were used in this study in the analysis of signals from multi-grain aliquots of each sediment sample. Figure 6 (*left column*) shows the change in  $D_e$  value with time integrals of optical stimulation for an aliquot from each sediment sample. Within this stimulation period two trap types, having contrasting bleaching efficiencies when exposed to blue-green (laboratory) optical stimulation, dominate the production of luminescence. If both trap types had been thoroughly reset prior to sample burial, then the slower bleaching trap

(dominating the latter 8-9 s of luminescence signal stimulation) should yield  $D_e$  values statistically concordant with those of the fast bleaching trap (dominating the initial 1-2 s of stimulation). Such 'flat'  $D_e(t)$  curves, as shown for sample GL03109 in Figure 6 (*left column*), may indicate that any residual signal present within grains of these aliquots as a result of partial bleaching is negligible compared with the total signal accrued subsequent to burial and may therefore evidence the accuracy of the associated  $D_e$  value. In contrast,  $D_e(t)$  curves exhibiting a statistically significant increase in  $D_e$  as stimulation period progresses, as in the case of two aliquots within samples GL03110 and GL03111 (Fig 6, *right column*), may indicate the presence of partially bleached grains.

Three intrinsic measures were used to confirm rising  $D_e(t)$  curves evolved owing to the presence of partially bleached grains rather than from internal mechanisms (Bailey *et al* 2003). Firstly, in order to confirm the sensitivity of  $D_e(t)$  analysis in detecting the presence of residual signals for these samples, partial bleaching by blue-green light has been simulated by administering a known laboratory dose to each sample and exposing each aliquot to a brief (4 s) blue-green (laboratory) optical stimulation (Bailey *et al* 2003). Following preheating, the remnant optical signal was measured and monitored for sensitivity change as described in section 2.3.1. The composition of the remnant signal should be dominated by emissions from the slower bleaching trap, the faster bleaching trap having been preferentially eroded of signal by the short optical stimulation which immediately followed irradiation. Substituting the remnant signal for the natural signal in Figure 2 (*left column, inset*), enables the  $D_e$  of the remnant signal to be calculated. The change in  $D_e$  with optical stimulation time can then be assessed. All aliquots of each sample exhibited rising  $D_e(t)$  as a result of simulated partial bleaching (Fig 6, *right column*).

The signal emanating from the slower bleaching trap may be artificially increased through aliquot preheating (Watanuki *et al* 2003) generating an artificial increase in  $D_e(t)$ . In order to confirm the absence of this internal effect for aliquots exhibiting rising  $D_e(t)$ , zero dose responses were substituted for the natural signal in Figure 2 (*left column, inset*) and  $D_e(t)$  plots constructed. The absence of a statistically significant increase in  $D_e(t)$ , for aliquots of GL03110 and GL03111 exhibiting rising  $D_e(t)$  derived from natural signals, confirms that the impact upon  $D_e(t)$  of preheat induced alterations in signal levels is negligible.

The final intrinsic measure of  $D_e(t)$  sensitivity in detecting partially bleached grains draws upon repeat regenerative-dose data. By substituting the repeat regenerative-dose signal for the natural dose in Figure 2 (*left column, inset*) for each aliquot, fully bleached grains are simulated and  $D_e(t)$  response can be monitored, the expectation being that each aliquot should exhibit a flat  $D_e(t)$  plot. This expectation is not fulfilled for those aliquots of GL03110 (Fig 6, *right column*) that displayed rising  $D_e(t)$  associated with natural signals. The implication of this feature is that an internal mechanism may have generated the rise in natural  $D_e(t)$  rather than the externally forced mechanism of partial bleaching. In contrast, aliquots of sample GL03111 describing rising  $D_e(t)$  from natural signals show no statistically significant increase in  $D_e(t)$  generated from repeat regenerative-dose data.

Therefore, given the presence of rising  $D_e(t)$  associated with both the natural signal and laboratory simulation of partial bleaching and absence of rising  $D_e(t)$  associated with both zero and repeat regenerative-dose data, aliquots within sample GL03111 likely contain partially bleached grains. Through construction of  $D_e(t)$  plots for individual aliquots, those containing a significant number of partially bleached grains can be distinguished from those composed of well-bleached grains and rejected from the dataset resulting in an amended  $D_e$  value enhanced in accuracy (Table 2). However, for the multi-grain aliquots of GL03111 this adjustment in mean  $D_e$  results in an insignificant alteration in age estimate.

The primary *caveat* associated with this signal analysis method of detecting partial bleaching is its dependence upon the pre-burial light spectrum exposure of a sample. If for the grains within an aliquot the dominant wavelengths of light causing a reduction in signal prior to burial were short (UV-violet), then the contrast in bleaching efficiency between trap types would have been minimal. Thus a distinction in  $D_e$  between each trap type may not be apparent, generating a 'flat'  $D_e(t)$  plot, yet each may contain an equivalent residual signal from partial bleaching due to insufficient exposure to sunlight. The sedimentary environment within which this signal analysis method is most sensitive is generally sub-aqueous contexts, within which the longer (>blue) wavelengths of sunlight dominate. However, given the spectrum of light exposure of each sample prior to burial cannot be defined categorically, the possibility that the flat  $D_e(t)$  plots yielded by aliquots of GL03109 and GL03110 reflect insensitivity of this signal analysis method in detecting partial bleaching, rather than the absence of partially bleached grains, cannot be dismissed.

### 3.2 Burnt Flint samples

The datable luminescence signal in flint is associated with the thermoluminescence peak at 380°C and the complete removal of this signal requires a firing temperature of ~450°C. An estimation of the firing temperature of burnt flint prior to burial can be made through signal analysis, comparing the natural and additive-dose thermoluminescence response. Such a comparison is illustrated in Figures 3 and 4 (*left column*) where the ratio of natural thermal signal to additive-less-natural thermal signal (Aitken 1985) is described for each sample. If the firing temperature prior to interment were sufficient for complete removal of the 380°C thermal signal then a plateau in ratio values should exist for the breadth of heating between 350°C to 450°C.

From Figure 3 (*left column*), sample GL03112 does not exhibit a plateau in ratios within the diagnostic region (350°C to 450°C), instead it describes a statistically significant increase in TL ratio from c 380°C onwards which may be indicative of a final firing temperature of <380°C. For sample GL03113, a statistically significant increase in ratios occurs between 350°C and 400°C, in contrast to the plateau in ratios between 400°C and 460°C. The ratio of natural and additive TL for sample GL03114 describes a plateau between 350°C and 400°C followed by a statistically significant increase in ratios between 420°C and 460°C, intimating a final firing temperature of <420°C. Sample GL03115 exhibits a trend of increasing TL ratios beyond 340°C, with pre-burial firing potentially occurring at less than this temperature. GL03116, whilst outlining a plateau in TL ratios within the diagnostic region, is characterised by a chaotic dose response curve, likely attributable to signal saturation resulting from little or no firing prior to burial. The TL ratios of GL03117 broadly describe a plateau between 380°C and 460°C indicating a final firing temperature >460°C.

In summary, samples GL03114 and GL03117, in exhibiting a plateau in TL ratios within the diagnostic region, likely received sufficient heating prior to burial to evolve  $D_e$  values representative of the burial period. Evidence of sufficient heating prior to burial for sample GL03113, based on ratios of natural to additive TL, is equivocal. This diagnostic alone cannot inform on the accuracy of the  $D_e$  value associated with this sample. However, the age estimate for GL03113 is coeval with GL03117, and is contemporary with the Mesolithic period, consistent with the expected age premised upon the range of microliths previously identified at this level. The age generated from GL03113 should at least be

considered as a maximum estimate. GL03112 and GL03115, in displaying a trend of increasing TL ratio with increasing temperature, appear to have received insufficient heating prior to burial, which would likely lead to  $D_e$  overestimation. Ages derived from these samples should only be considered maximum estimates. In light of a saturated dose response, GL03116 appears to have received little or no heating prior to interment and is not considered further in this study.

#### 4.0 Discussion

Optical age estimates from sediment samples are stratigraphically consistent, exhibiting a statistically significant increase in age with sample depth. Further, the optical age of the uppermost sediment sample and is coeval with those derived from two proximal charcoal samples subjected to AMS radiocarbon dating (Fig 1 and Fig 5). Of those thermoluminescence age estimates accepted in the previous section (GL03113, GL03114, and GL03117), all are contemporary with the Mesolithic period and therefore consistent with age expectations founded upon microliths previously identified at equivalent levels across the site.

However, a stratigraphic discordance exists between age estimates derived from sediment sample GL03111 (*c* 32 ka) and the underlying burnt flint sample GL03117 (*c* 12 ka). Determining the origin of this discordance between independent metrics of age requires consideration of the relative influence of potential internally and externally forced inaccuracies for each technique.

Considering the burnt flint ages as underestimates; inherent effects forcing this inaccuracy can be contemplated in terms of  $D_e$  underestimation and/or overestimation of dose rate. For the former, the accuracy of  $D_e$  extrapolations was evaluated using regenerative-dose responses (Figs 3 and 4, *right column*). No inaccuracy associated with each chosen model of  $D_e$  extrapolation is apparent. Dose rate overestimation may originate from an underestimation of average moisture content. Sediment samples associated with burnt flint samples GL03114 to GL03117, supplied by the client for quantification of external  $\gamma$  dose rate, yielded moisture contents lower than those evaluated from sediment samples collected for optical dating by this laboratory, perhaps evidencing evaporation of moisture within sediment samples supplied by the client. However, even if a moisture content approximating saturation fraction (*c* 40% dry weight) is incorporated into external  $\gamma$  dose rate calculations, the resulting adjustment in flint age estimates is statistically insignificant.

An externally forced mechanism of age underestimation may relate to the stratigraphic impersistence of flint samples. One (GL03117) or all flints may have been translocated downwards either instantaneously through anthropogenic activity or over the period of burial through gravitational effects coupled with a lack of adhesion afforded by the coarse sand matrix dominating below ~0.60m. The timing of such displacement of flints will affect the rate of cosmic dose exposure, which is in part modulated by the thickness of overburden. Given that cosmic dose rate contributes significantly to total dose rate (up to c 50%), its variation requires consideration. Whilst the timing of a potential flint displacement cannot be quantified, a minimum and maximum estimation of cosmic dose rate can be approximated, and the impact upon age estimates evaluated. A minimum cosmic dose rate can be defined by flint displacement and accumulation of overburden occurring shortly after burial. Effectively this characterises the conditions assumed in quantifying cosmic dose rate within the age estimates presented in Table 2 and Figure 5. Maximum cosmic dose rate can be defined by flint displacement and overburden accumulation occurring long after burial, relative to the burial period. In Figure 5, the adjustment in age resulting from incorporation of a maximum cosmic dose rate value, quantified by assuming all samples remained buried yet close to the surface for the majority of their burial period, is statistically insignificant relative to ages incorporating a minimum value for the cosmic dose rate. Therefore, temporal variations in cosmic dose rate because of displacement of datable material or variations in the thickness of overburden will not have a statistically significant impact upon luminescence age estimates.

Considering the sediment ages as overestimates, inherent sources of such inaccuracy may relate to  $D_e$  overestimation and/or dose rate underestimation. In respect of the former condition, partial bleaching of each sediment sample's datable signal has been considered by means of signal analysis. No significant effect upon  $D_e$  estimation, by insufficient pre-burial sunlight exposure, was detected using this diagnostic. However, detection of partial bleaching using multi-grain aliquot signal analysis is not infallible. Further assurance of adequate pre-burial bleaching may stem from a future quantification of inter-grain  $D_e$  distributions, the shape of which may diagnose the origin of post-burial signals and inform on the accuracy of the sediment age estimates derived (Murray and Roberts 1997; Murray *et al* 1995). Underestimation of dose rate through overestimation of average moisture content can be quantified by incorporating dry dose rate values into the age equation. The result is a statistically insignificant adjustment in optical age. As discussed above and illustrated in Figure 5, the effect of cosmic dose rate underestimation upon optical age

estimates can be quantified by considering a maximum cosmic dose rate value. Again the impact upon age estimates is negligible.

A further discordance in age estimates can be observed within the uppermost dated unit comprising the last appearance and highest concentration of microliths. Whilst the sediment and charcoal fragments indicate an age of c 2.8 ka, the burnt flint sample GL03113 generates one significantly older (c 10.3 ka). The consistency in ages generated by independent chronometric signals testifies to the accuracy of the optical and radiocarbon estimates. However, age overestimation by GL03113 is doubtful given evidence of sufficient pre-burial heating (section 3.2) and consistency in age with that of the microliths based on typology. Therefore, the discrepancy in age of materials within the uppermost unit is likely symptomatic of a reactivation of this land surface. An initial period of activity during the Mesolithic is indicated by microliths typology and burnt flint age estimates whose time dependent (thermal) signal once reset by firing was preserved within the flint core. The land surface then remained relatively stable until the Iron Age where charcoal was formed and incorporated; the optical signal of the sediments being reset contemporaneously through sunlight exposure during anthropogenic and/or pedogenic reworking.

## **5.0 Conclusions**

Of the intrinsic and extrinsic factors considered, the age inversion between sediment sample GL03111 and flint sample GL03117 has likely resulted from a displacement of the flint from its primary context. The mode and timing of translocation cannot be established, however. The consistency of sediment age estimates with sample location, coupled with evidence of sufficient bleaching prior to burial supplied by signal analysis, may be indicative of accurate age determination. The accuracy of the upper optical age estimate is further supported by AMS radiocarbon dating of the same unit. However, conclusions on the degree of pre-burial bleaching for the lower sediment samples may be further adjudged through acquisition of single grain  $D_e$  values.

Given the current data set, sediment located within 1.55 m to 1.35 m of section A11 accumulated some time between c 33 ka (31,000 BC) and 23 ka (21,000 BC). Sediment located between 1.35 m and 0.59 m was deposited some time between c 23 ka and 2.8 ka (800 BC); flints located within this sediment, exhibiting evidence of sufficient heating prior to burial, may further resolve the age of these sediments to c 7-10 ka (5000 – 8000 B.C.).

However these flint samples may be afflicted by displacement from primary context as has been intimated for GL03117. The juxtaposition of Mesolithic burnt flints and Iron Age sediments and charcoal in the uppermost dated unit evidences a period of land surface stability and repeated occupation. Sediments located at and above 0.59 m accumulated at and possibly after c 2.8 ka (800 BC).

Laboratory Code	Grain size ( $\mu\text{m}$ )	Moisture content	Nal $\gamma$ -spectrometry ( <i>in situ</i> )			Total $\gamma$ dose rate ( $\text{Gy.ka}^{-1}$ )	ICP-MS Analysis			Total $\alpha$ dose rate ( $\text{Gy.ka}^{-1}$ )	Total $\beta$ dose rate ( $\text{Gy.ka}^{-1}$ )	Cosmic Dose Rate ( $\text{Gy.ka}^{-1}$ )	Total Dose Rate ( $\text{Gy.ka}^{-1}$ )	Mean		Amended Mean	
			K (%)	Th (ppm)	U (ppm)		K (%)	Th (ppm)	U (ppm)					$D_e$ (Gy)	Age (ka)	$D_e$ (Gy)	Age (ka)
GL03109	125-180	$0.06 \pm 0.01$	$0.16 \pm 0.01$	$1.95 \pm 0.12$	$0.81 \pm 0.08$	$0.22 \pm 0.01$	$0.22 \pm 0.00$	$2.26 \pm 0.02$	$0.67 \pm 0.01$	-	$0.28 \pm 0.01$	$0.19 \pm 0.02$	$0.69 \pm 0.03$	$1.93 \pm 0.08$	$2.8 \pm 0.2$	-	-
GL03110	125-180	$0.08 \pm 0.02$	$0.00 \pm 0.00$	$0.94 \pm 0.09$	$0.53 \pm 0.06$	$0.10 \pm 0.01$	$0.01 \pm 0.00$	$1.23 \pm 0.01$	$0.24 \pm 0.01$	-	$0.06 \pm 0.00$	$0.17 \pm 0.02$	$0.34 \pm 0.02$	$7.65 \pm 0.60$	$22.8 \pm 2.2$	-	-
GL03111	125-180	$0.11 \pm 0.03$	$0.01 \pm 0.09$	$1.00 \pm 0.10$	$0.33 \pm 0.06$	$0.09 \pm 0.02$	$0.02 \pm 0.00$	$0.85 \pm 0.01$	$0.19 \pm 0.00$	-	$0.05 \pm 0.00$	$0.16 \pm 0.02$	$0.30 \pm 0.03$	$9.63 \pm 0.63$	$32.1 \pm 3.6$	$9.74 \pm 0.67$	$32.5 \pm 3.8$
			ICP-MS Analysis (associated sediment)				ICP-MS Analysis (flint)										
			K (%)	Th (ppm)	U (ppm)		K (%)	Th (ppm)	U (ppm)								
GL03112	125-180									$0.06 \pm 0.01$	$0.06 \pm 0.00$		$0.39 \pm 0.02$	$7.87 \pm 1.79$	$20.1 \pm 4.7$	-	-
GL03113	125-180	$0.07 \pm 0.02$	$0.02 \pm 0.00$	$1.08 \pm 0.02$	$0.23 \pm 0.01$	$0.08 \pm 0.00$	$0.04 \pm 0.00$	$0.18 \pm 0.01$	$0.21 \pm 0.01$	$0.07 \pm 0.02$	$0.07 \pm 0.00$	$0.19 \pm 0.02$	$0.41 \pm 0.02$	$4.22 \pm 0.44$	$10.3 \pm 1.2$	-	-
GL03114	125-180									$0.08 \pm 0.02$	$0.07 \pm 0.00$		$0.37 \pm 0.02$	$2.42 \pm 0.59$	$6.6 \pm 1.6$	-	-
GL03115	125-180	$0.01 \pm 0.00$	$0.01 \pm 0.00$	$0.39 \pm 0.01$	$0.17 \pm 0.01$	$0.04 \pm 0.00$	$0.03 \pm 0.00$	$0.17 \pm 0.01$	$0.25 \pm 0.00$	$0.09 \pm 0.02$	$0.07 \pm 0.00$	$0.18 \pm 0.02$	$0.37 \pm 0.02$	$21.86 \pm 7.25$	$58.5 \pm 19.8$	-	-
GL03116	125-180									-	-		-	-	-	-	-
GL03117	125-180	$0.02 \pm 0.00$	$0.02 \pm 0.00$	$0.57 \pm 0.01$	$0.22 \pm 0.00$	$0.06 \pm 0.00$	$0.02 \pm 0.00$	$0.08 \pm 0.00$	$0.18 \pm 0.01$	$0.06 \pm 0.01$	$0.05 \pm 0.00$	$0.16 \pm 0.02$	$0.32 \pm 0.02$	$4.01 \pm 0.30$	$12.5 \pm 1.3$	-	-

**Table 2** Dosimetry,  $D_e$  and age data obtained during luminescence dating of the Bletchingley Mesolithic deposits. Moisture content expressed as a fraction of wet weight. Flint  $\alpha$  dose rate calculation incorporates an a-value of  $0.10 \pm 0.02$ .

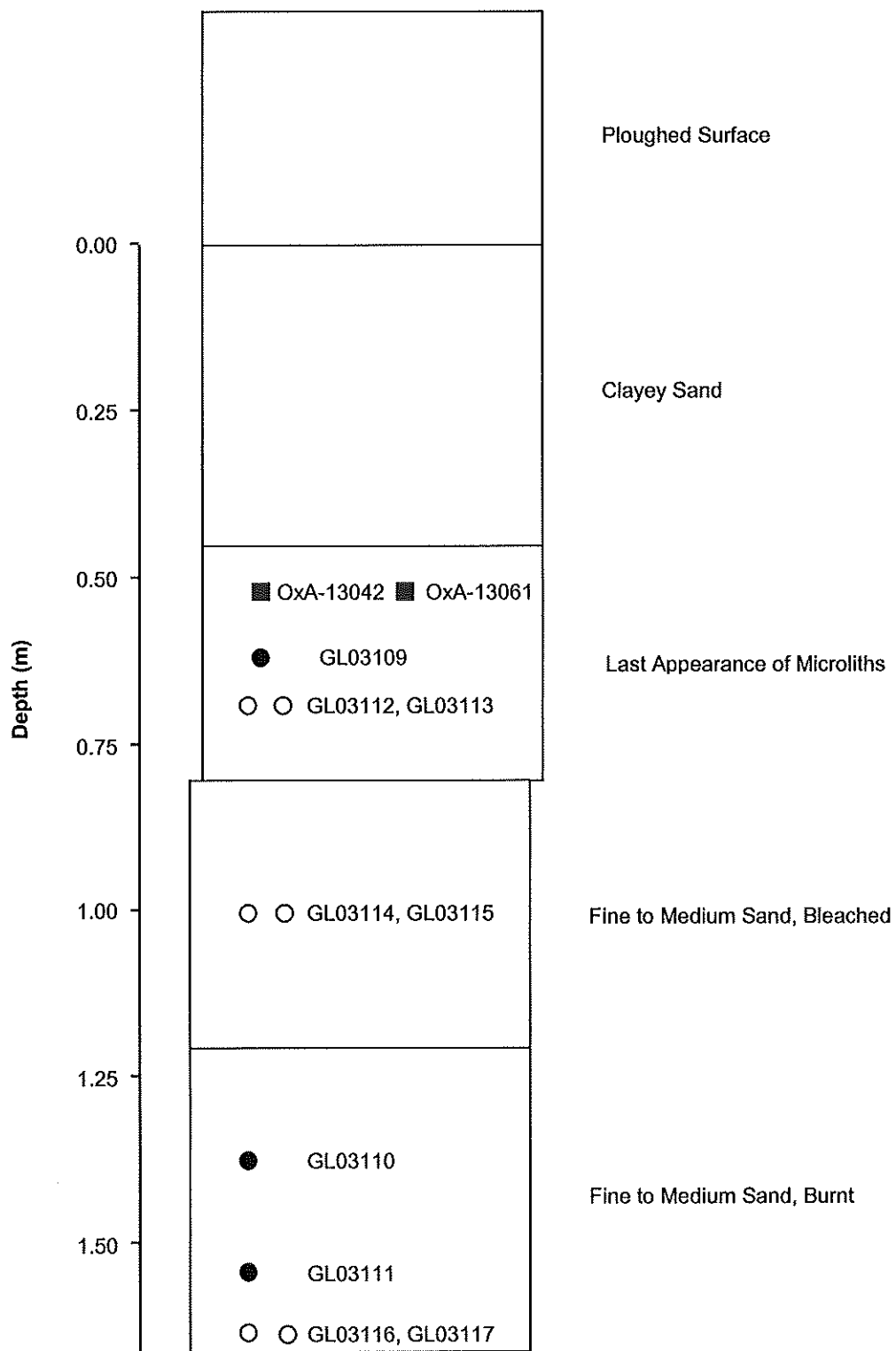


**Figure 1**

Section A11 showing the locations of sediment samples taken for optical dating (filled circles), burnt flint samples for thermoluminescence dating (unfilled circles) and charcoal for AMS radiocarbon dating.

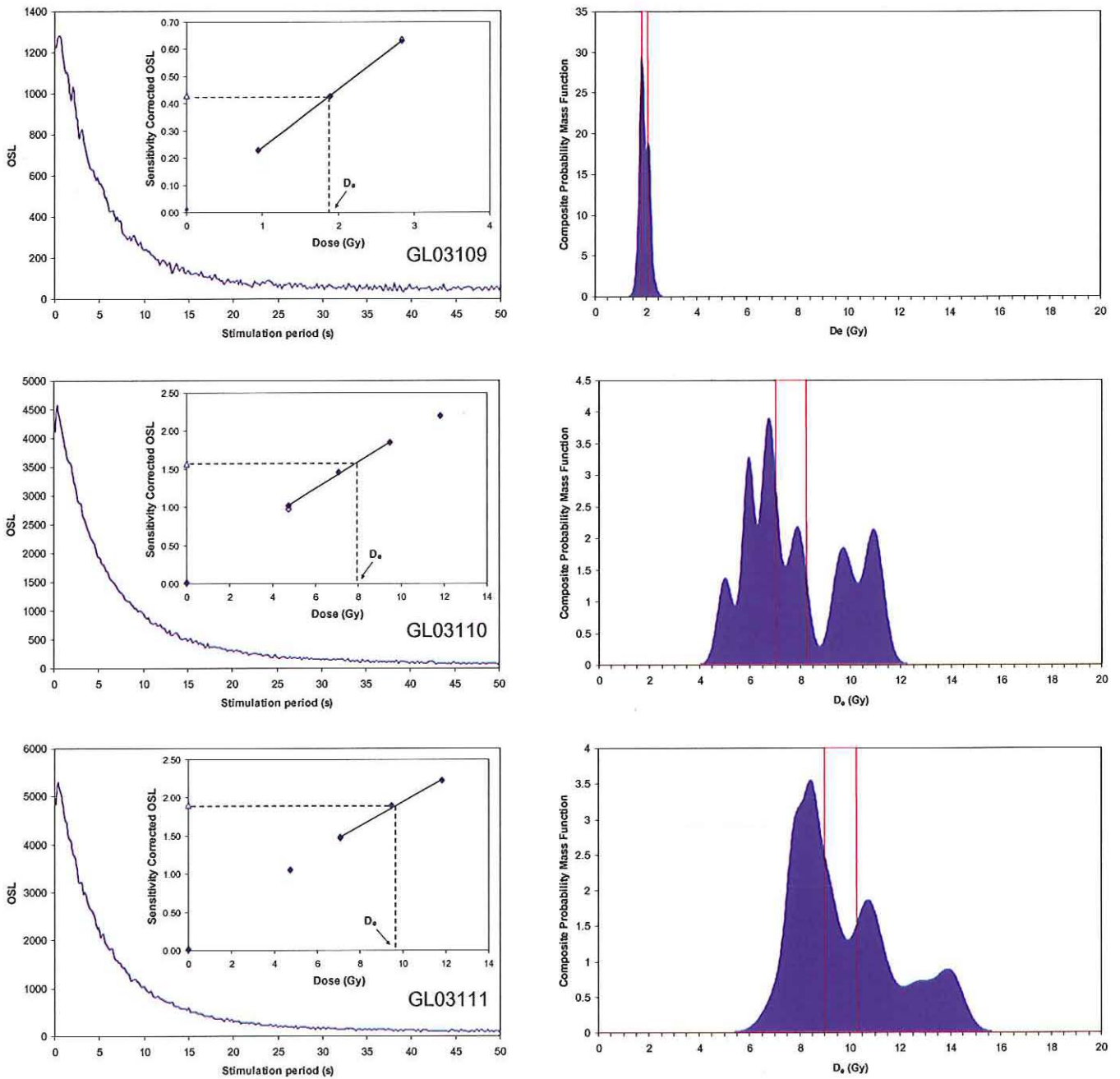


**Figure 2** *Left column*, example of natural optical signals within quartz extracts of conventional optical dating samples taken from section A11, listed in stratigraphic order. *Inset*, example of sensitivity corrected optical response to dose and interpolation of  $D_e$  value, the natural signal denoted by an open triangle, regenerative-dose signals by filled diamonds, and repeat regenerative-dose response by an open diamond. *Right column*, composite probability mass function showing the multi-grain aliquot  $D_e$  estimates generated by each sample. Red delimits the  $1\sigma$  standard error range about the geometric mean  $D_e$  value

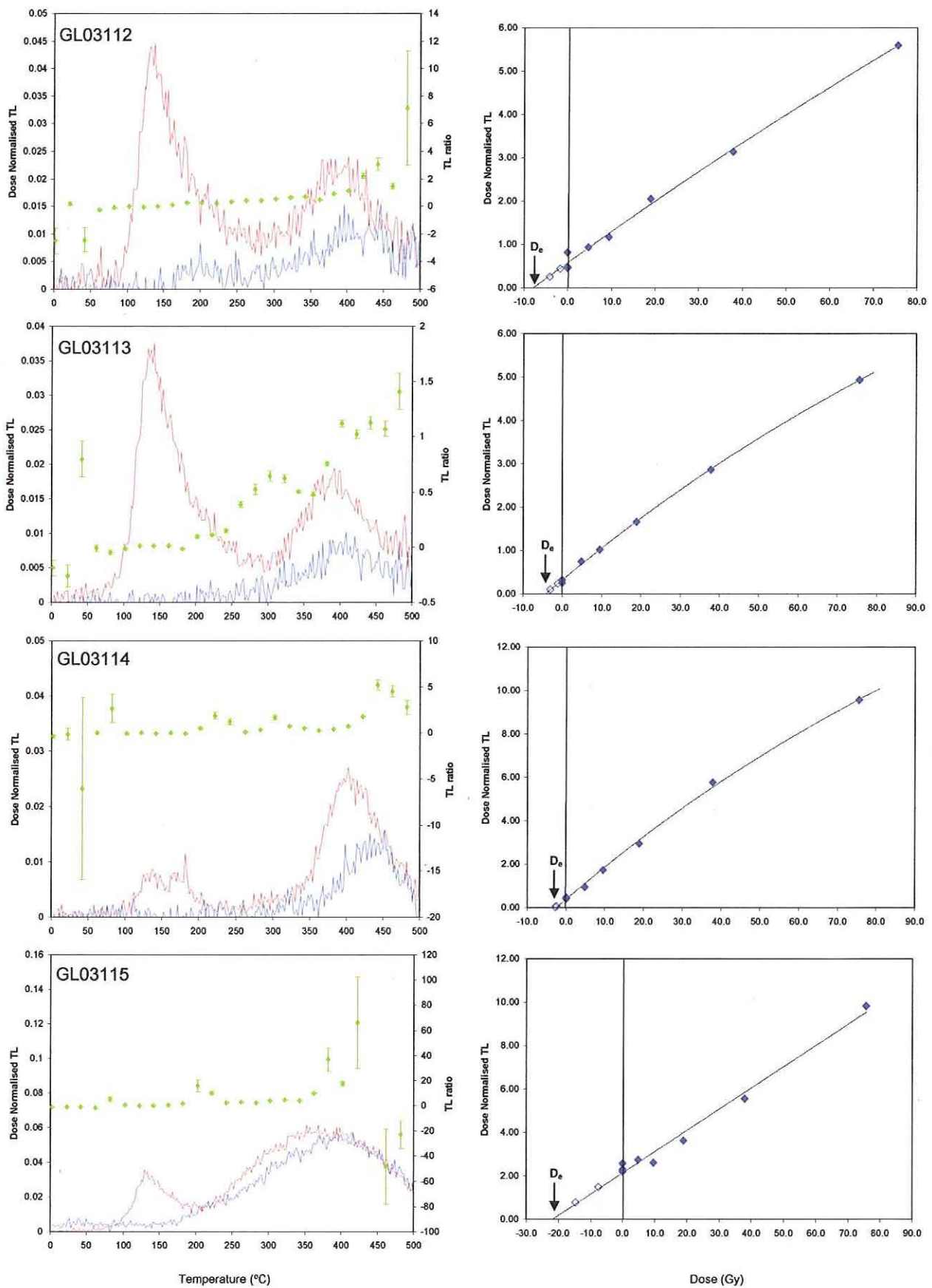


**Figure 3** *Left column*, natural (in blue) and additive (in red) dose TL response of flint samples with an approximation of sufficient heating prior to burial evidenced by a plateau in natural to additive TL ratios (in green) between 350°C and 450°C. *Right column*, additive dose response curves illustrating  $D_e$  extrapolation

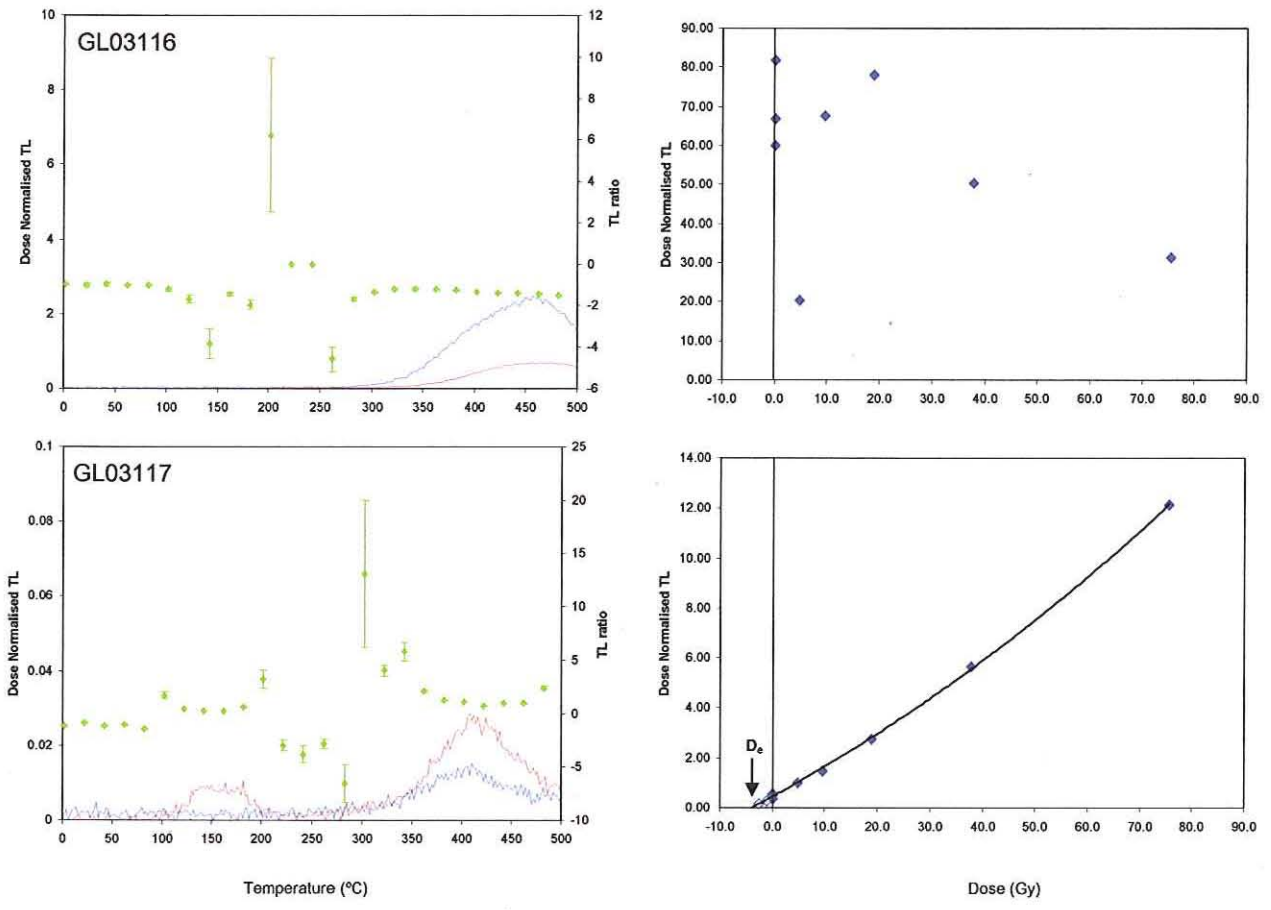


**Figure 4** *Left column*, natural (in blue) and additive (in red) dose TL response of flint samples with an approximation of sufficient heating prior to burial evidenced by a plateau in natural to additive TL ratios (in green) between 350°C and 450°C. *Right column*, additive dose response curves illustrating  $D_e$  extrapolation

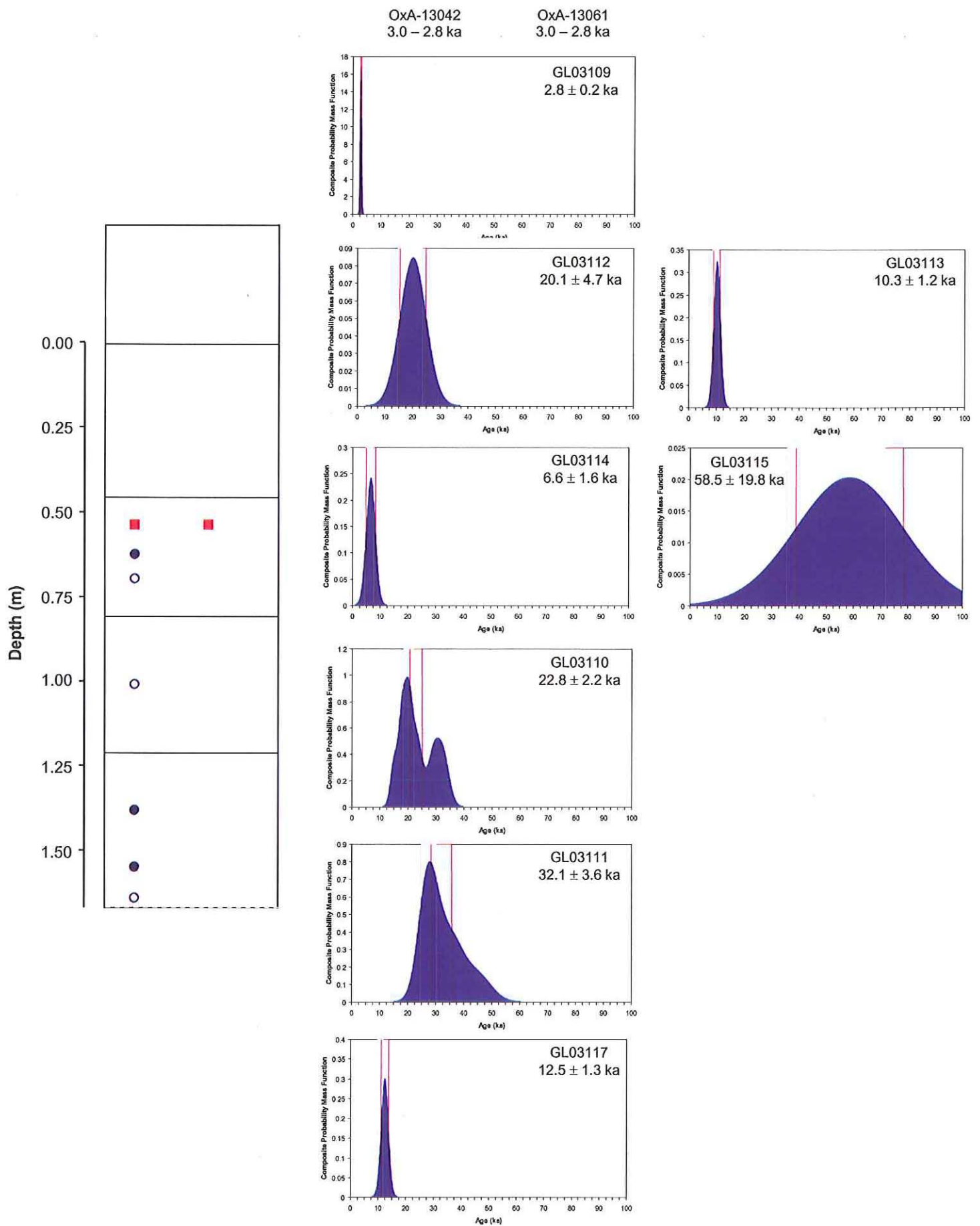


**Figure 5** Section log and composite probability mass functions of ages generated by multi-grain aliquots of sediment and burnt flint samples, arranged in stratigraphic order. Red delimits the mean age and  $1\sigma$  standard error range. Grey delimits the mean age and  $1\sigma$  standard error range incorporating a maximum cosmic dose rate value ( $0.214 \text{ Gy}\cdot\text{ka}^{-1}$ , equating to near surface sample location for majority of burial period). AMS  $^{14}\text{C}$  ages are calibrated, derived from the 95% confidence probability range.

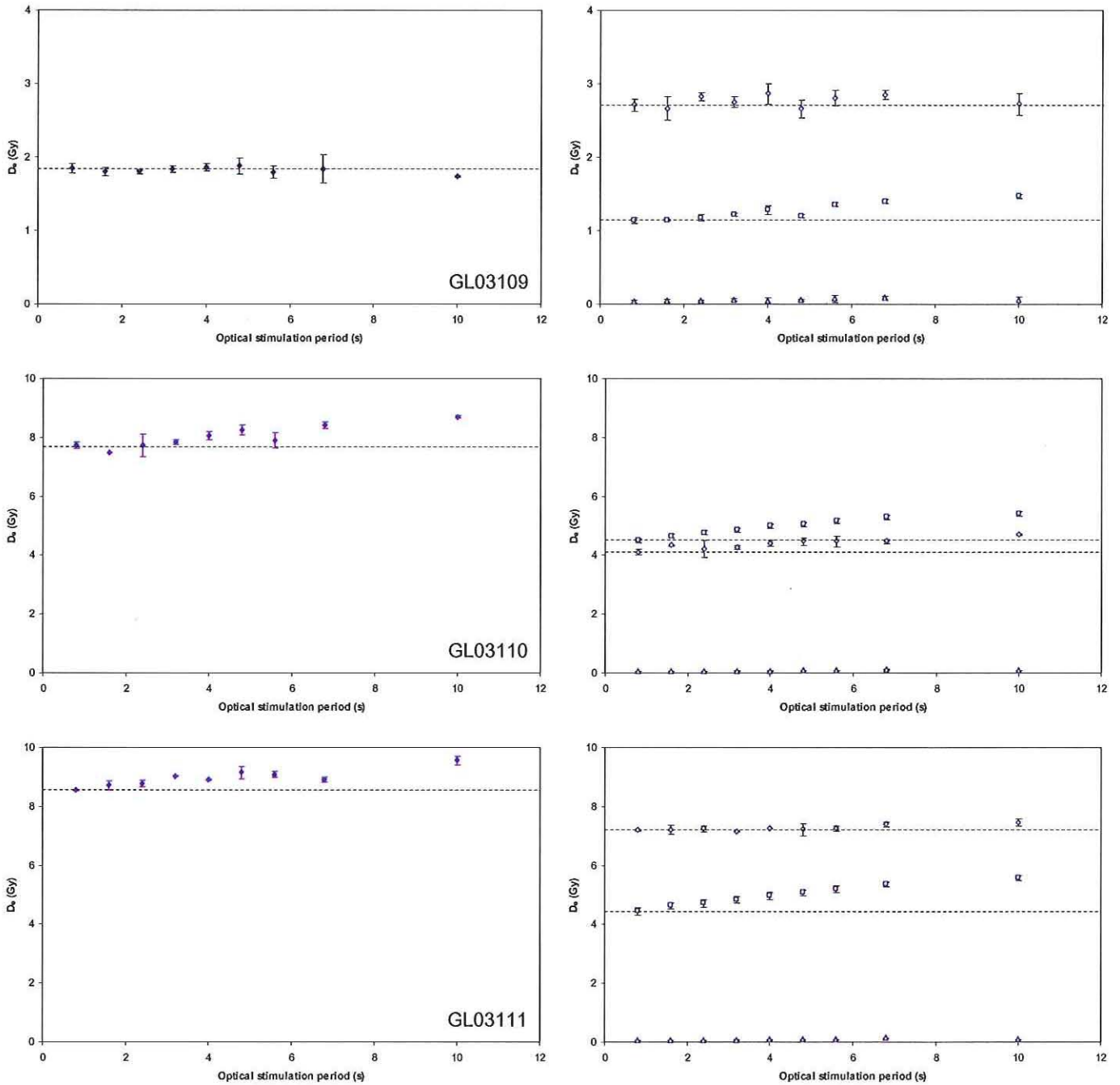


**Figure 6** *Left column*,  $D_e(t)$  plots of variation in natural  $D_e$  of aliquots of Bletchingley sediment samples as a function of optical stimulation time. Rising  $D_e(t)$  plots may indicate the presence of partially bleached grains. Flat  $D_e(t)$  plots reflect either negligible levels of partial bleaching relative to the dose accrued during burial or insensitivity of this signal analysis method in detecting partial bleaching. *Right column*, intrinsic measures of sensitivity of  $D_e(t)$  plots in detecting partial bleaching through simulation of partial bleaching (open squares), quantification of preheat induced effects upon  $D_e(t)$  (open triangles) and simulation of full bleaching (open diamonds); see section 3.1 for explanation

## References

- Adamiec, G, and Aitken, M J, 1998 Dose-rate conversion factors: new data, *Ancient TL*, **16**, 37-50
- Aitken, M J, 1985 *Thermoluminescence dating*, London (Academic Press)
- Bailey, R M, 2003 Paper I: The use of measurement-time dependent single-aliquot equivalent-dose estimates from quartz in the identification of incomplete signal resetting, *Radiation Measurements*, **37**, 673-83
- Bailey, R M, Singarayer, J S, Ward, S, and Stokes, S, 2003 Identification of partial resetting using  $D_e$  as a function of illumination time, *Radiation Measurements*, **37**, 511-18
- Bell, W T, 1979 Thermoluminescence dating: radiation dose-rate data, *Archaeometry*, **21**, 243-45
- Bowman, S G E, 1982 Thermoluminescence studies on burnt flint, *PACT*, **6**, 353-61
- Galbraith, R F, Roberts, R G, Laslett, G M, Yoshida, H, and Olley, J M, 1999 Optical dating of single and multiple grains of quartz from Jinmium rock shelter (northern Australia): Part I, Experimental design and statistical models, *Archaeometry*, **41**, 339-64
- Green, J R, and Margerison, D, 1978 *Statistical treatment of experimental data*, New York (Elsevier Scientific Publications)
- Hütt, G, Jaek, I, and Tchonka, J, 1988 Optical dating: K-feldspars optical response stimulation spectra, *Quat Sci Rev*, **7**, 381-86
- Huxtable, J, 1981 Light bleaching of archaeological flint samples: a warning, *Ancient TL*, **16**, 2-4
- Markey, B G, Bøtter-Jensen, L, and Duller, G A T, 1997 A new flexible system for measuring thermally and optically stimulated luminescence, *Radiation Measurements*, **27**, 83-9

- Mejdahl, V, 1979 Thermoluminescence dating: beta-dose attenuation in quartz grains, *Archaeometry*, **21**, 61-72
- Mercier, N, Valladas, H, and Valladas, G, 1995 Flint thermoluminescence dates from the CFR laboratory at GIF: contributions to the study of the chronology of the Middle Palaeolithic, *Quat Sci Rev*, **14**, 351-64
- Murray, A S, and Olley, J M, 2002 Precision and accuracy in the Optically Stimulated Luminescence dating of sedimentary quartz: a status review, *Geochronometria*, **21**, 1-16
- Murray, A S, and Roberts, R G, 1997 Determining the burial time of single grains of quartz using optically stimulated luminescence, *Earth Planetary Sci Letters*, **152**, 163-80
- Murray, A S, and Wintle, A G, 2000 Luminescence dating of quartz using an improved single-aliquot regenerative-dose protocol, *Radiation Measurements*, **32**, 57-73
- Murray, A S, and Wintle, A G, 2003 The single aliquot regenerative dose protocol: potential for improvements in reliability, *Radiation Measurements*, **37**, 377-81
- Murray, A S, Olley, J M, and Caitcheon, G G, 1995 Measurement of equivalent doses in quartz from contemporary water-lain sediments using optically stimulated luminescence, *Quat Sci Rev*, **14**, 365-71
- Murray, A S, Wintle, A G, and Wallinga, J, 2002 Dose estimation using quartz OSL in the non-linear region of the growth curve, *Radiation Protection Dosimetry*, **101**, 371-4
- Prescott, J R, and Hutton, J T, 1994 Cosmic ray contributions to dose rates for luminescence and ESR dating: large depths and long-term time variations, *Radiation Measurements*, **23**, 497-500
- Smith, B W, Rhodes, E J, Stokes, S, Spooner, N A, 1990 The optical dating of sediments using quartz, *Radiation Protection Dosimetry*, **34**, 75-8
- Spooner, N A, 1993 The validity of optical dating based on feldspar, unpublished D Phil thesis, Oxford Univ

Stokes, S, Ingram, S, Aitken, M J, Sirocko, F, and Anderson, R, 2003 Alternative chronologies for late Quaternary (Last Interglacial-Holocene) deep sea sediments via optical dating of silt-sized quartz, *Quat Sci Rev*, **22**, 925-41

Templer, R H, 1985 The removal of anomalous fading in zircons, *Nuclear Tracks Radiation Measurements*, **10**, 531-7

Valladas, H, 1978 Thermoluminescence dating of burnt stone from a prehistoric site, *PACT*, **2**, 180-3

Valladas, G, 1988 Stopping power and range for alpha particles in SiO<sub>2</sub>, *Ancient TL*, **6**, 7-8

Wallinga, J, Murray, A S, Duller, G A T, and Tornqvist, T E, 2001 Testing optically stimulated luminescence dating of sand-sized quartz and feldspar from fluvial deposits, *Earth Planetary Sci Letters*, **193**, 617-30

Watanuki, T, Murray, A S, and Tsukamoto, S, submitted Quartz and polymineral luminescence dating of Japanese loess over the last 0.5 Ma: comparison with an independent chronology, *Earth Planetary Sci Letters*

Watanuki, T, Murray, A S, Tsukamoto, S, 2003 A comparison of OSL ages derived from silt-sized quartz and polymineral grains from Chinese loess, *Quat Sci Rev*, **22**, 991–97

Wintle, A G, 1973 Anomalous fading of thermoluminescence in mineral samples, *Nature*, **245**, 143-4

Wintle, A G, and Aitken, M J, 1977 Thermoluminescence dating of burnt flint: application to a lower Palaeolithic site, Terra Amata, *Archaeometry*, **19**, 111-30

Zimmerman, D W, 1971 Thermoluminescent dating using fine grains from pottery, *Archaeometry*, **13**, 29-52